Supporting Information

1. General

The chemical reagents were supplied by commercial company (Aladdin LLC). The organic solvents were treated by standard anhydrous procedure before use. Pre-coated glass plates were applied for TLC analysis. Column chromatography was carried out on silica gel (200-300 mesh). NMR spectra were performed in the solvent of $CDCl_3$ or DMSO-d_6 on the Bruker-ARX 600 instrument at 26 ^oC. Bruker mass spectrometer was used for recording the MS spectra. Elemental analyses were analysed on Vario EL IIIElemental Analyzer. UV-Vis spectra were measured on Varian UV-Vis spectrometer. Fluorescence spectra were examined on the Hitachi F-4500 spectrometer. Compound **1** and **2a-2c** were prepared according to the literatures, respectively. (*Organic & Biomolecular Chemistry*, 2017, **15**, 6006-6013, and *J. Incl. Phenom. Macrocycl. Chem*., 2010, **67**, 49-54).

2. The synthetic process and characteristic spectra.

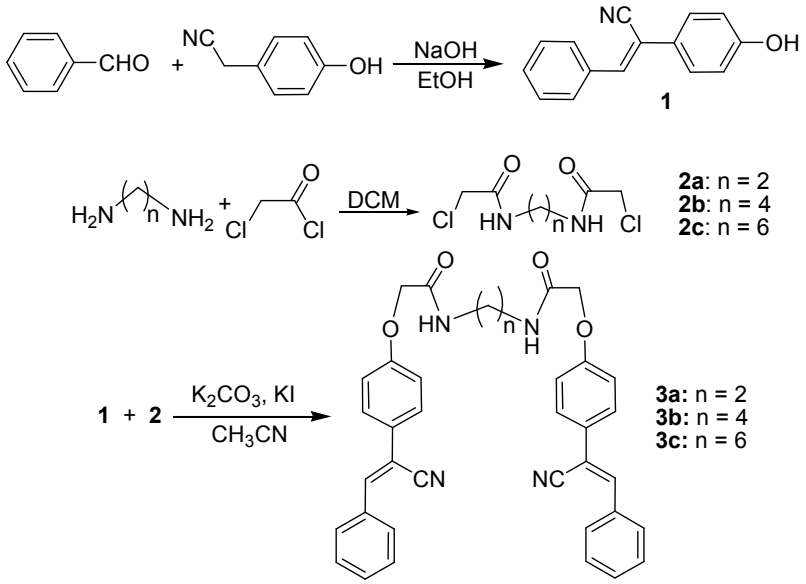

Scheme S1 The synthesis of compounds **3a**, **3b** and **3c**

2.1 Synthesis of compounds 3a, 3b and 3c.

Under N_2 atmosphere, the mixture of compound **1** (0.22 g, 1 mmol) and compound **2a** (**2b** or **2c**) (0.5 mmol) was stirred and refluxed in 20 mL of dry MeCN for 24 h with dry K_2CO_3 (0.41g, 3 mmol) and KI (0.10g, 0.6 mmol) as catalyst. The disappearance of starting materials was examined by TLC detection. Subsequently, 30 mL of HCl solution (1 M) and 30 mL of CH_2Cl_2 were added in reaction system under stirring. Then the mixture was partitioned and the organic layer was dried by anhydrous $MgSO_4$. The organic layer was further concentrated under reduced pressure. The residue was purified by rapid column chromatography (eluent: CH_2Cl_2). compounds **3a**, **3b** and **3c** were obtained as pale yellow solid in yields of 72%, 70% and 75%, respectively.

Compound **3a**: ^{1}H NMR (400 MHz, DMSO-d_6) δppm: 3.28 (s, 4H, NCH_2), 4.54(s, 4H, OCH_2), 7.09 (d, 4H, *J* = 8.0Hz,ArH), 7.29 (d, 4H, *J*= 8.0Hz, ArH), 7.43-7.53 (m, 4H, CH and ArH), 7.69 (d, 4H, *J* = 8.0Hz,ArH), 7.90 (m, 4H, ArH), 8.26(s, 2H, NH); ^{13}C NMR (100 MHz, DMSO-d_6) δppm: 168.30, 158.92, 141.36, 134.35, 130.74, 130.42, 130.05, 129.38, 129.04, 127.65, 115.85, 110.36, 67.41, 55.34; MALDI-MS ($C_{36}H_{30}N_4O_4$) $[M]^+$: Calcd.: 582.227. found:605.195 $[M+Na]^+$; Anal. calcd for $C_{36}H_{30}N_4O_4$: C 74.21, H 5.19, N 9.62; found C 74.25, H 5.22, N 9.56%.

Compound **3b**: ^{1}H NMR (400 MHz, DMSO-d_6) δppm: 1.44(s, 4H, CH_2), 3.14 (s, 4H, NCH_2), 4.54(s, 4H, OCH_2), 7.09 (d, 4H, *J* = 8.0Hz, ArH), 7.29 (d, 4H, *J*= 8.0Hz, ArH), 7.47-7.54 (m, 4H, CH and ArH), 7.71 (d, 4H, *J* = 8.0Hz,ArH), 7.90 (t, 4H, *J* = 4.0Hz, ArH), 8.18(s, 2H, NH); ^{13}C NMR (100

MHz, DMSO-d_6) δppm: 167.64, 158.81, 141.45, 134.01, 130.76, 130.41, 130.06, 129.39, 129.05, 127.67, 115.85, 110.39, 67.49, 55.34, 26.96; MALDI-MS ($C_{38}H_{34}N_4O_4$) $[M]^+$: Calcd.: 610.258. found: 611.061$[MH]^+$; Anal. calcd for $C_{38}H_{34}N_4O_4$: C 74.73, H 5.61, N 9.17; found C 74.76, H 5.65, N 9.11%.

Compound **3c**: ^{1}H NMR (400 MHz, DMSO-d_6) δppm: 1.23(bs, 4H, CH_2), 1.41(bs, 4H, CH_2), 3.12 (bs, 4H, NCH_2), 4.50(s, 4H, OCH_2), 7.09 (d, 4H, *J* = 8.0Hz, ArH), 7.29 (d, 4H, *J*= 8.0Hz, ArH), 7.47-7.54 (m, 4H, CH and ArH), 7.71 (d, 4H, *J* = 8.0Hz,ArH), 7.91 (t, 4H, *J* = 4.0Hz, ArH), 8.11(s, 2H, NH); ^{13}C NMR (100 MHz, DMSO-d_6) δppm: 167.60, 158.77, 141.43, 133.96, 130.69, 130.40, 130.06, 129.37, 129.05, 127.65, 115.97, 113.11, 67.27, 56.52, 29.44, 26.42; MALDI-MS ($C_{40}H_{38}N_4O_4$) $[M]^+$: Calcd.: 638.289. found: 638.976$[M]^+$, 661.293$[M+Na]^+$; Anal. calcd for $C_{40}H_{38}N_4O_4$: C 75.21, H 6.00, N 8.77; found C 75.27, H 6.04, N 8.69%.

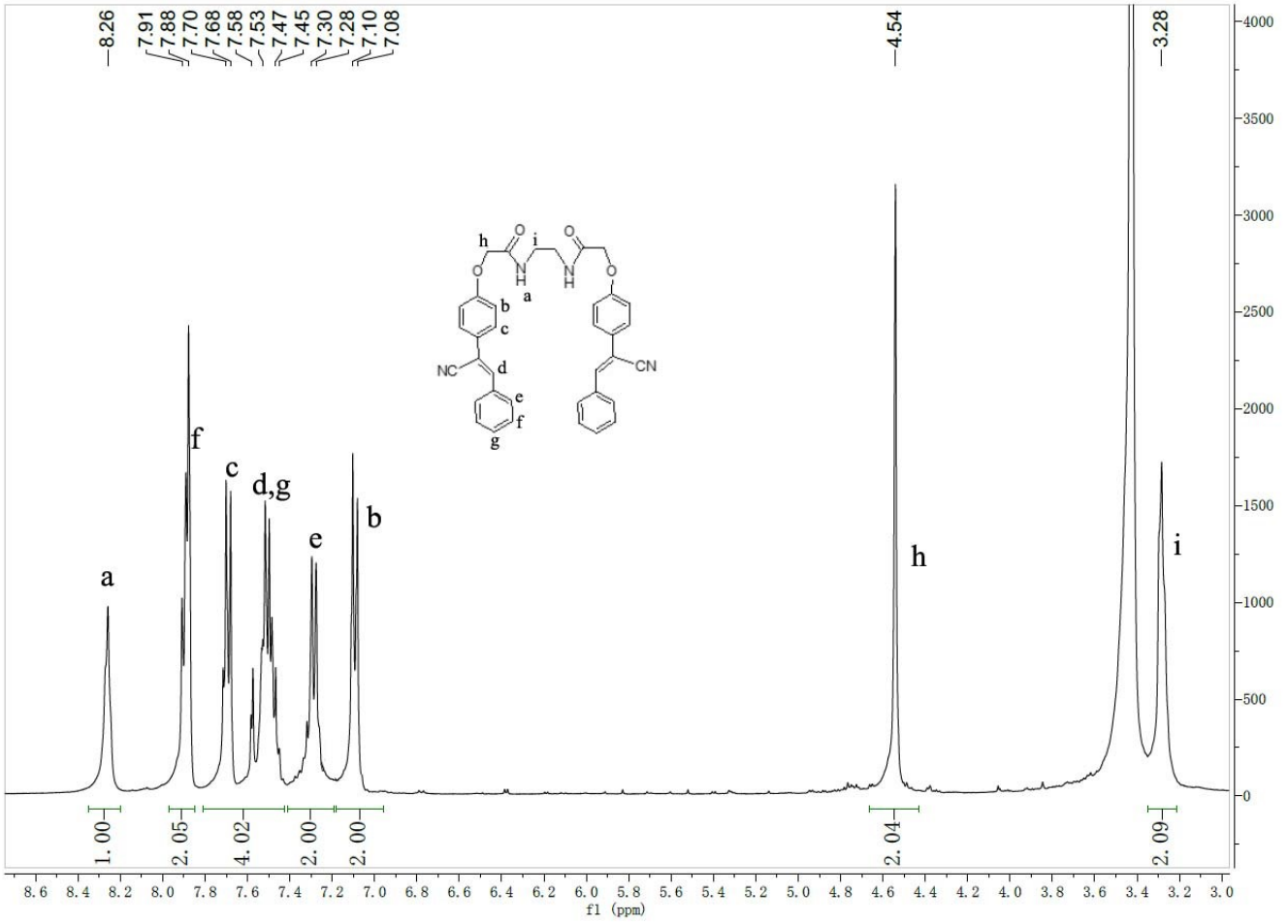

Figure S1. The ^{1}H NMR spectrum of compound **3a**

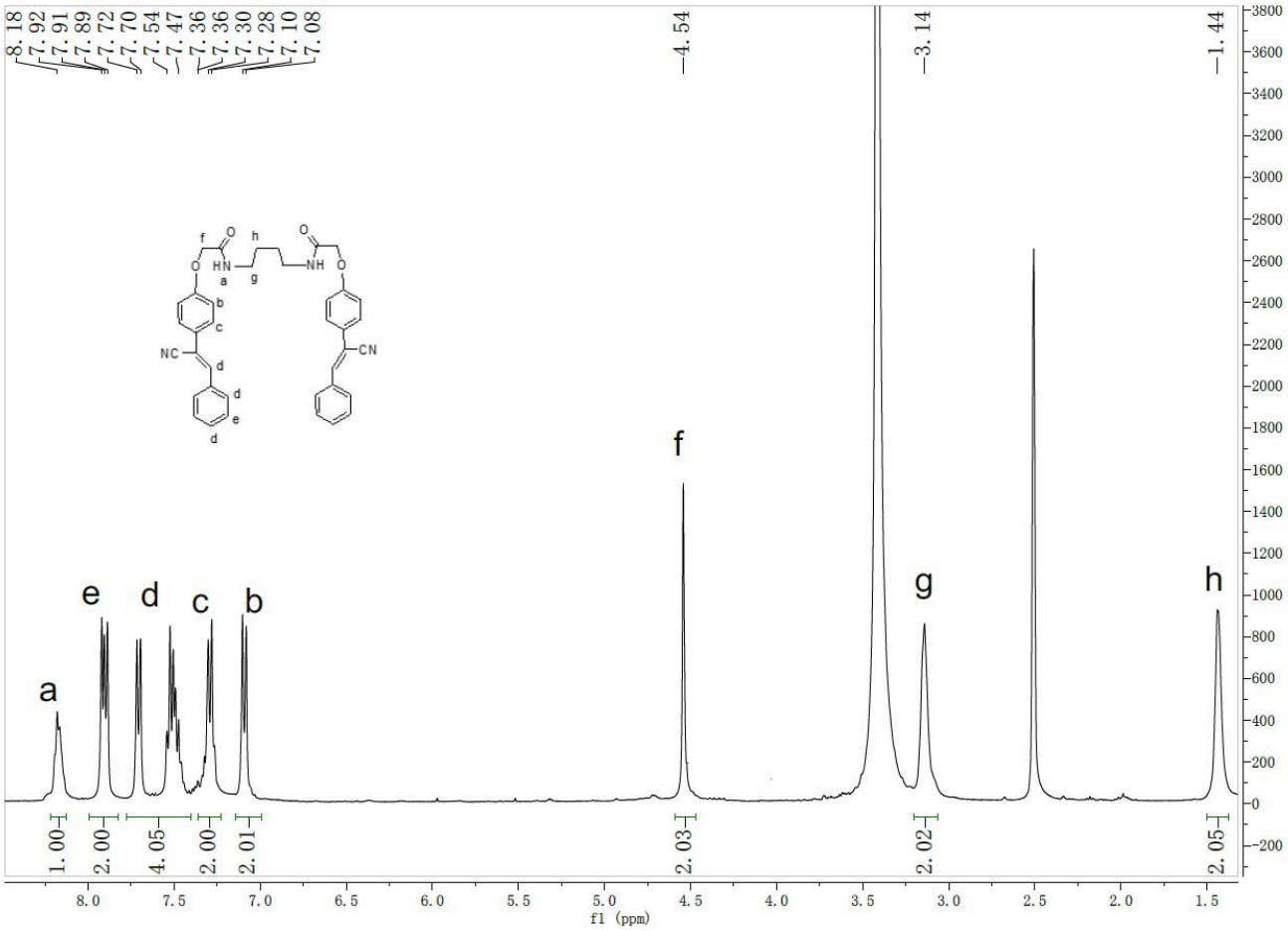

Figure S2. The ^{1}H NMR spectrum of compound **3b**

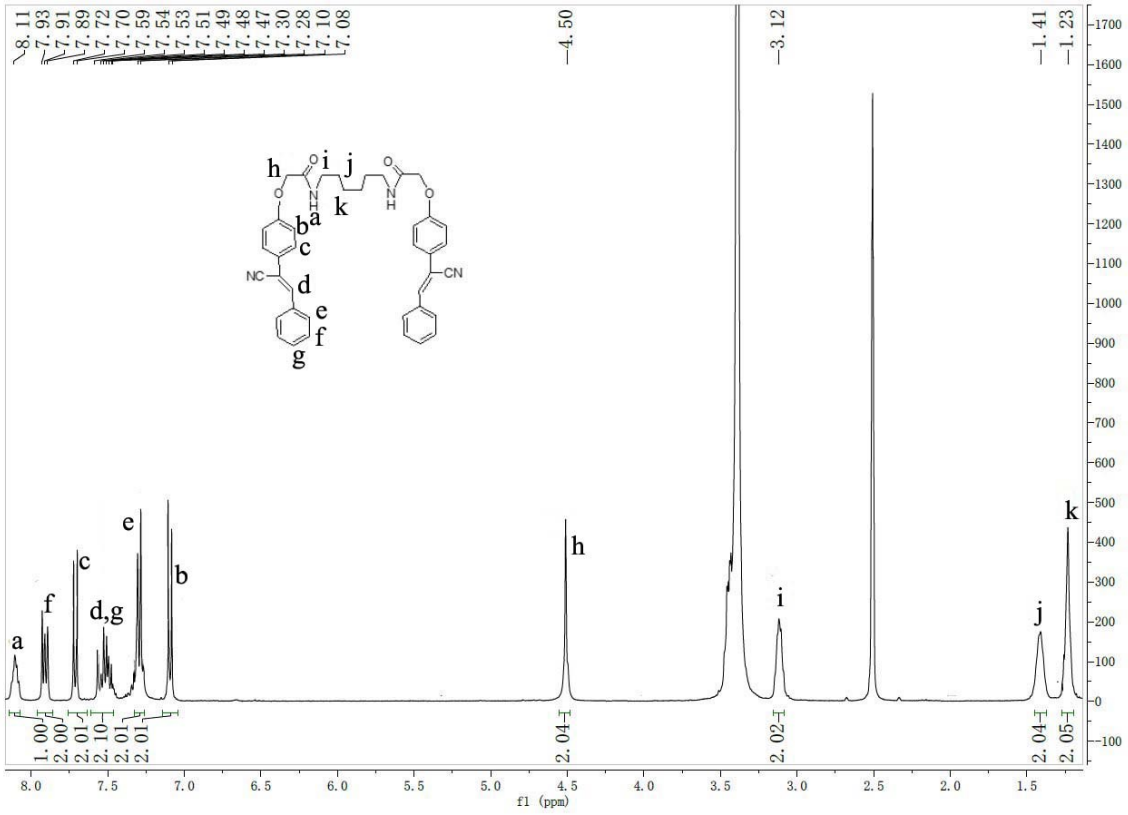

Figure S3. The ^{1}H NMR spectrum of compound **3c**

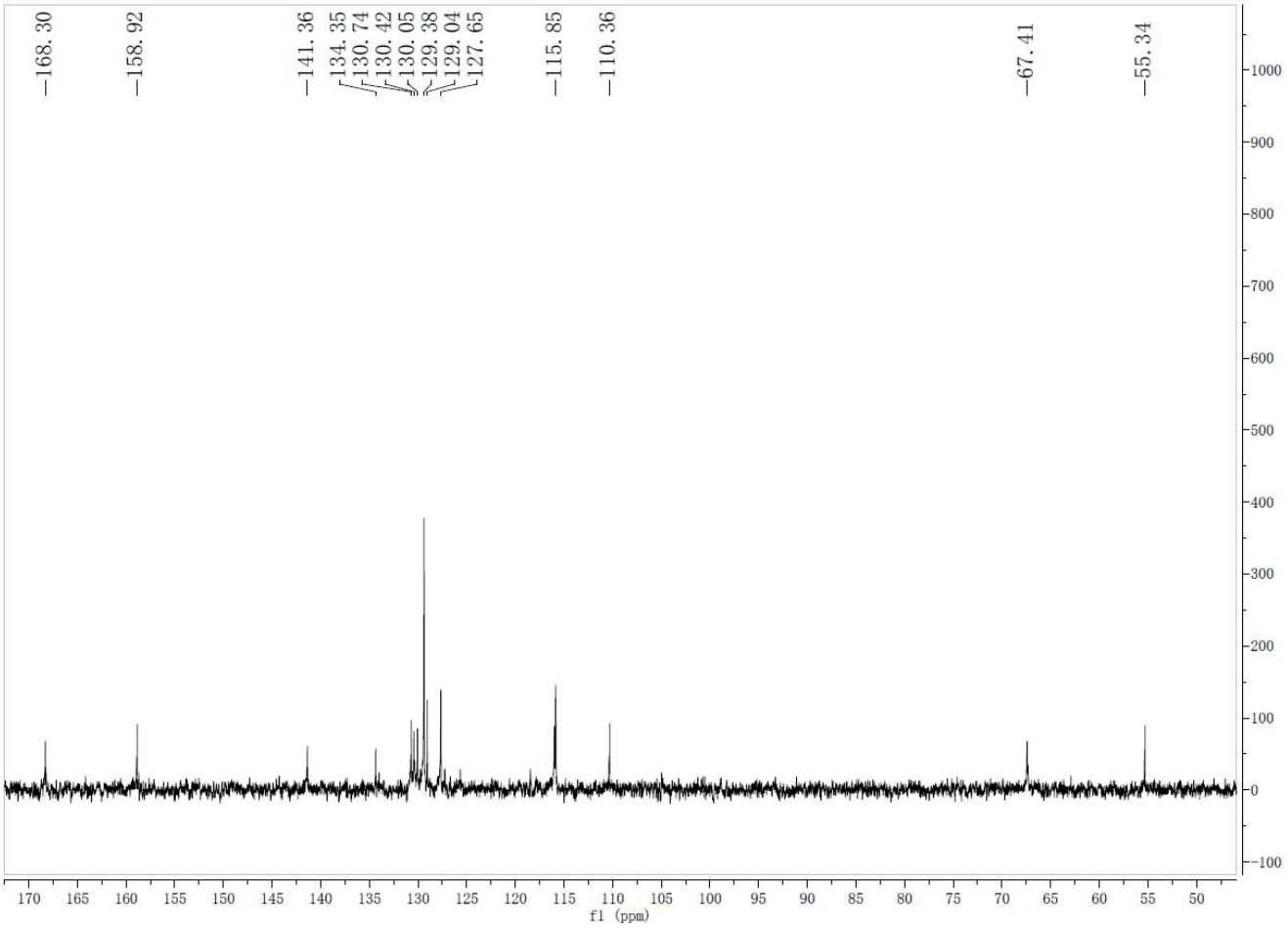

Figure S4. The ^{13}C NMR spectrum of compound **3a**

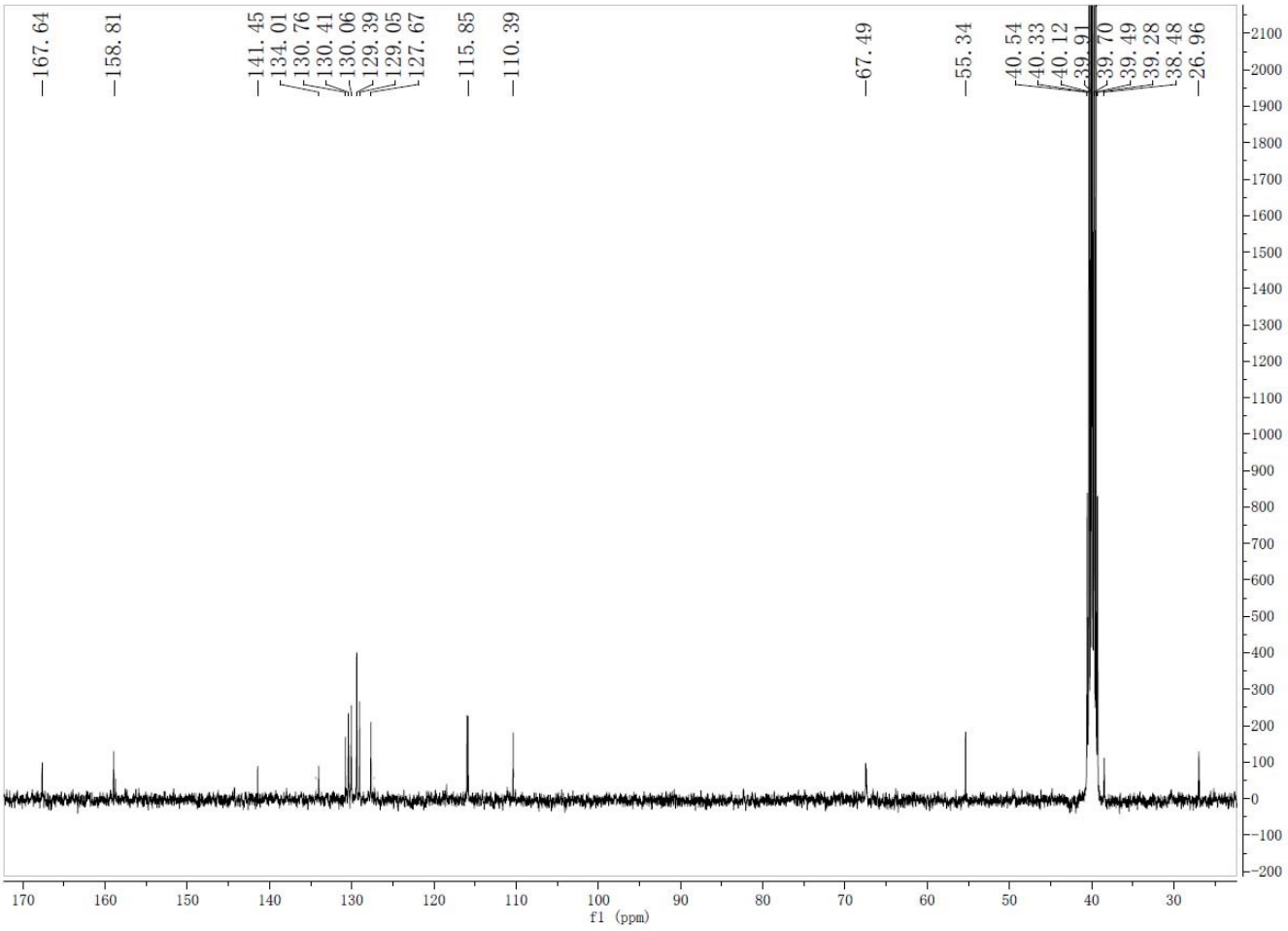

Figure S5. The ^{13}C NMR spectrum of compound **3b**

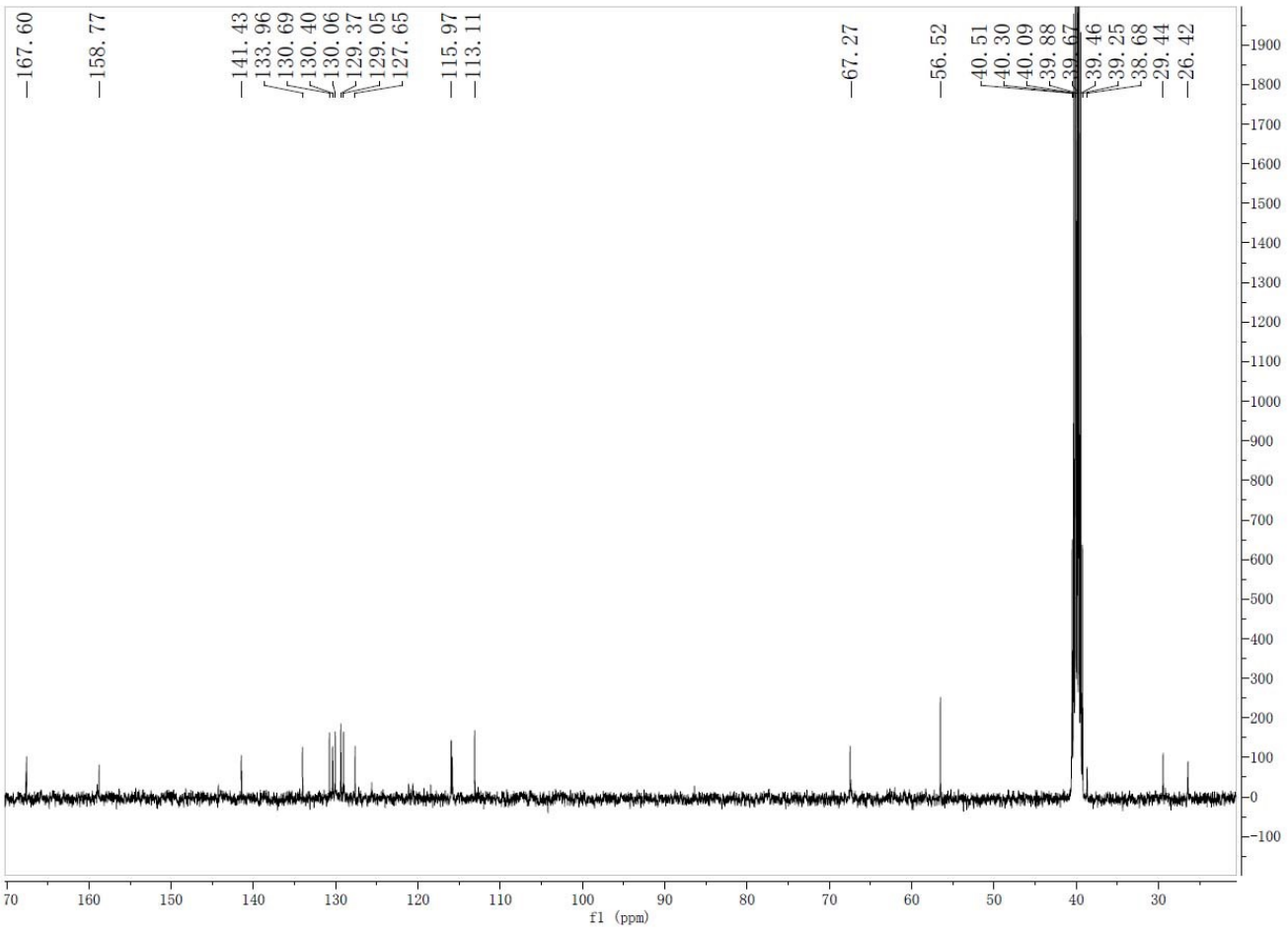

Figure S6. The ^{13}C NMR spectrum of compound **3c**

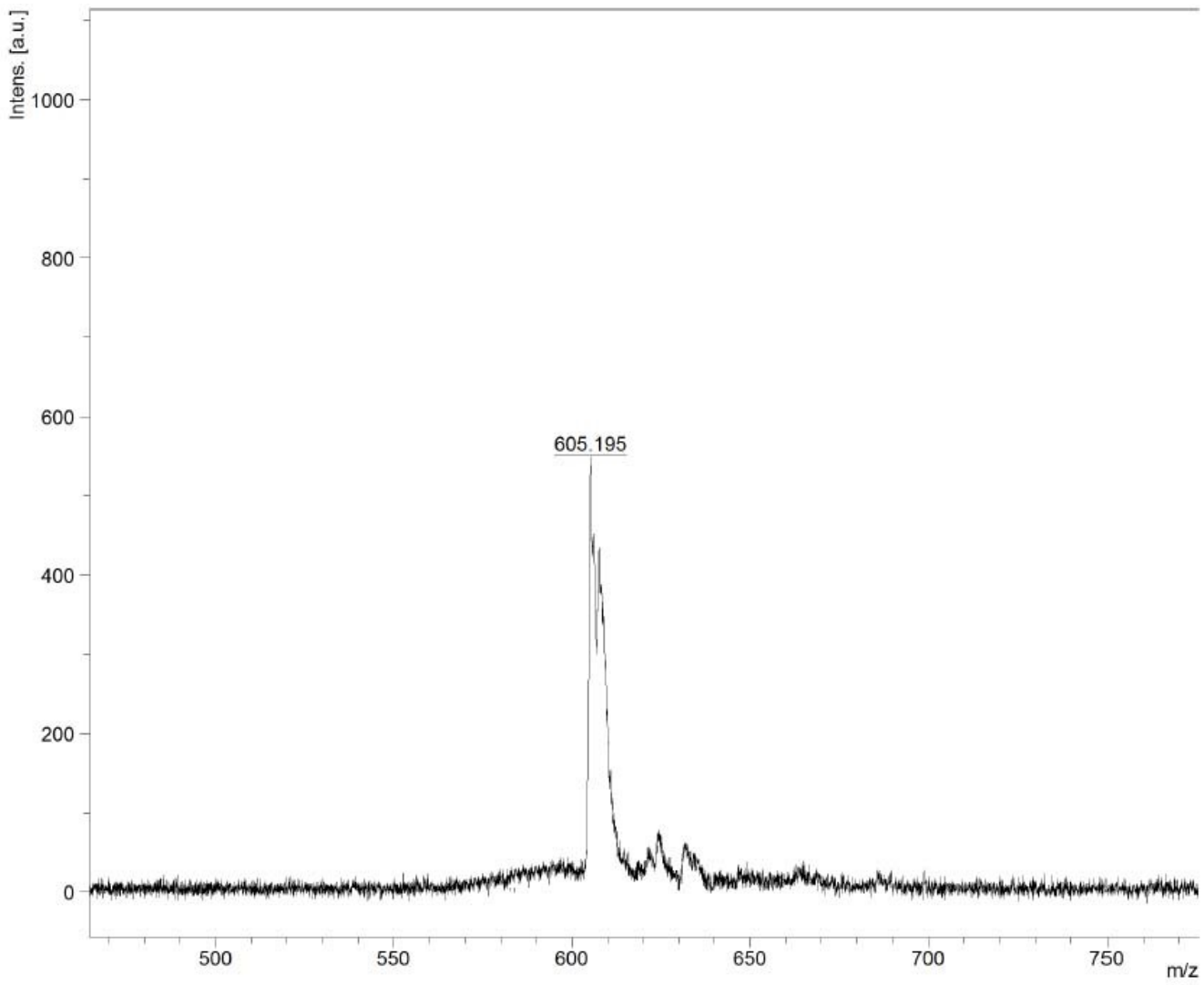

Figure S7. MALDI-MS spectrum of compound **3a**

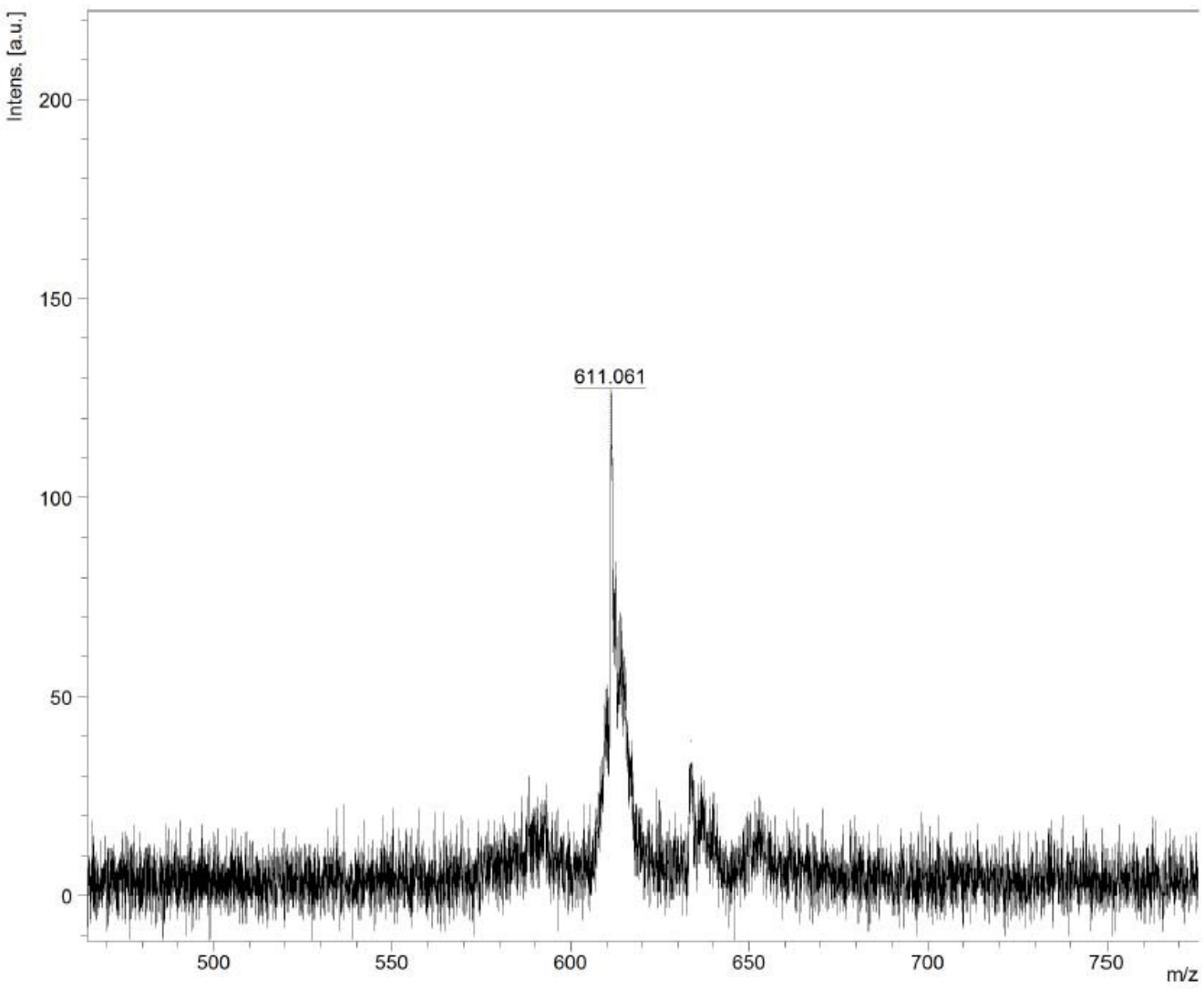

Figure S8. MALDI-MS spectrum of compound **3b**

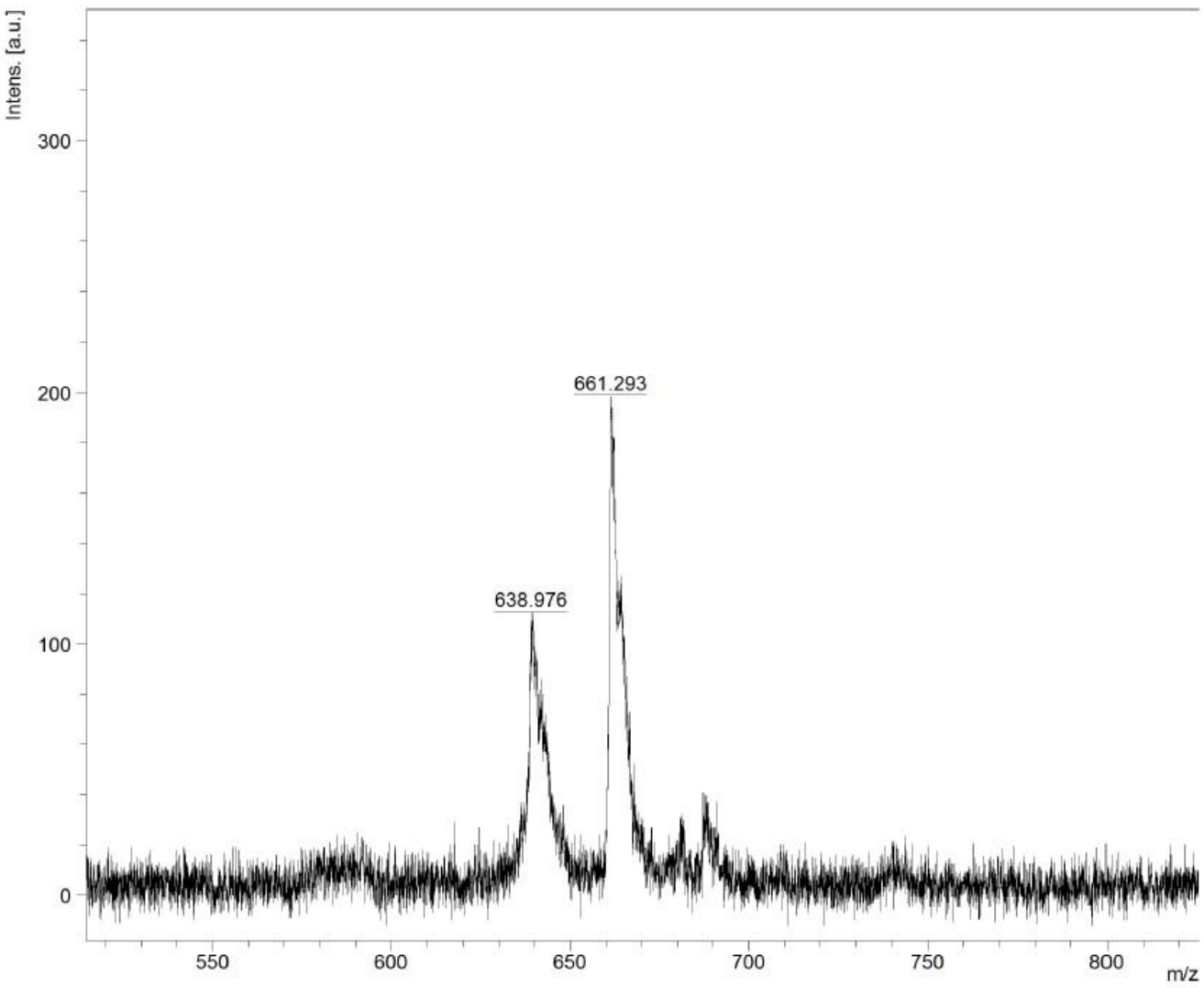

Figure S9. MALDI-MS spectrum of compound **3c**

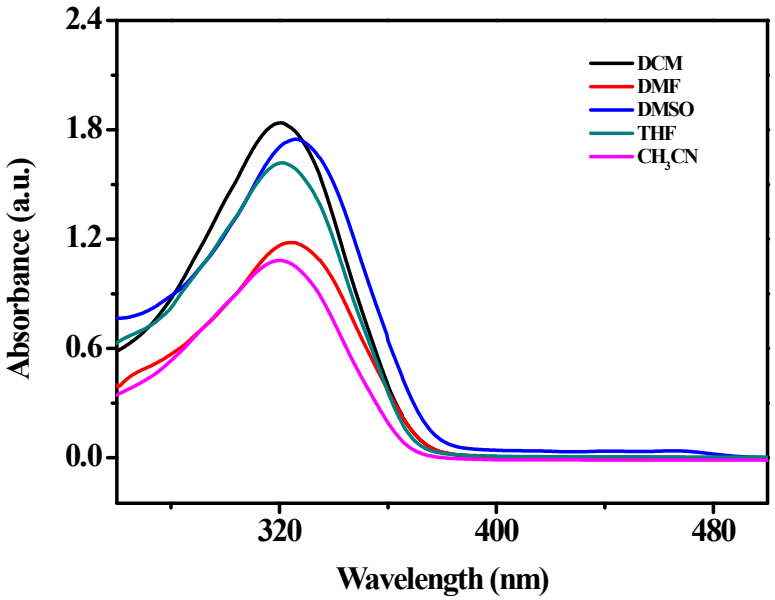

Figure S10 The UV-Vis absorption spectra of compound **3a** in different solvents (1.0×10^{-5} M)

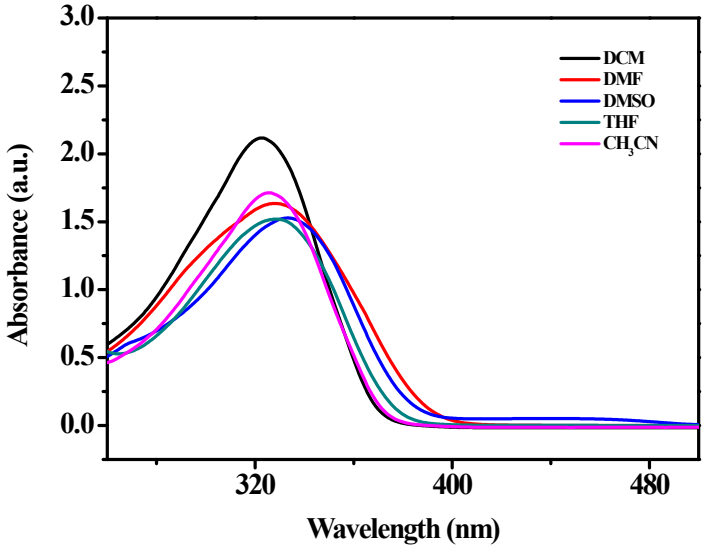

Figure S11 The UV-Vis absorption spectra of compound **3b** in different solvents (1.0×10^{-5} M)

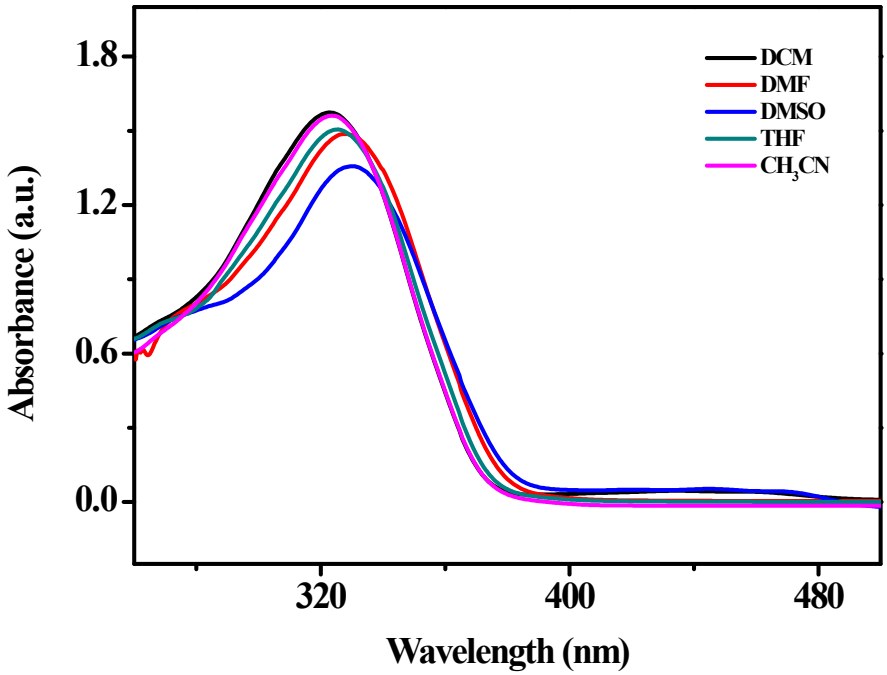

Figure S12 The UV-Vis absorption spectra of compound **3c** in different solvents (1.0×10^{-5} M)

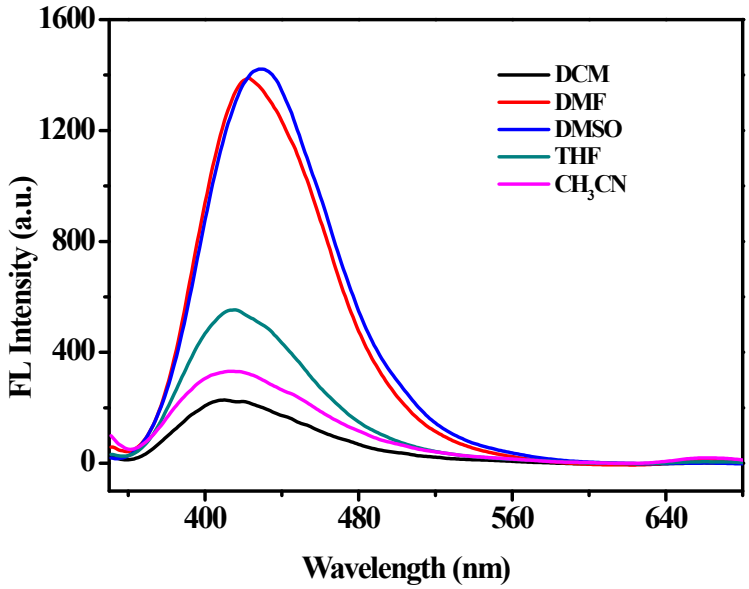

Figure S13 The emission spectra of compound **3a** in different solvents (1.0×10^{-5} M) with the excitation wavelength of 320 nm.

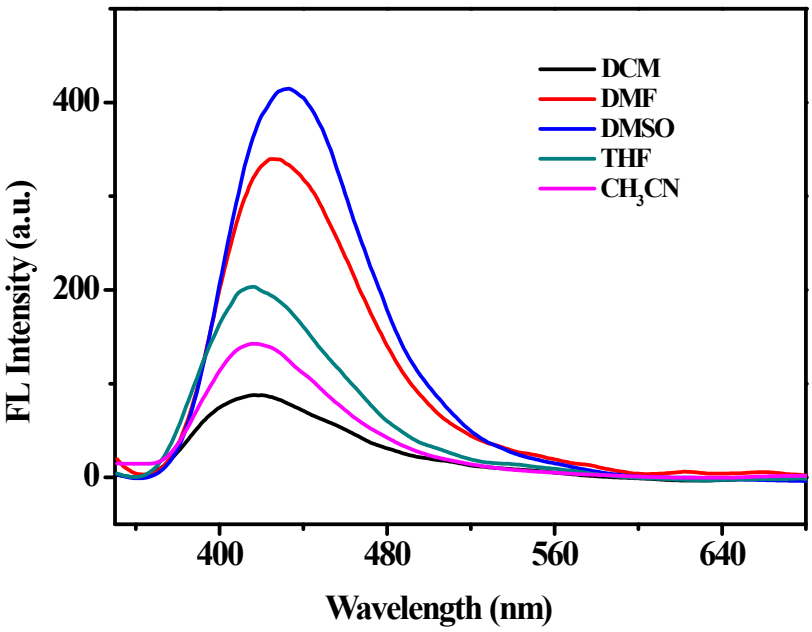

Figure S14 The emission spectra of compound **3b** in different solvents (1.0×10^{-5}M) with the excitation wavelength of 320 nm.

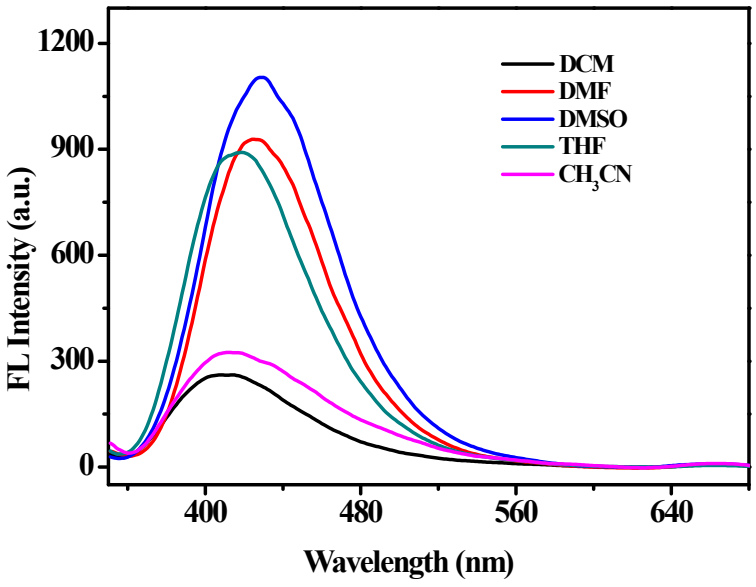

Figure S15 The emission spectra of compound **3c** in different solvents (1.0×10^{-5}M) with the excitation wavelength of 320 nm.

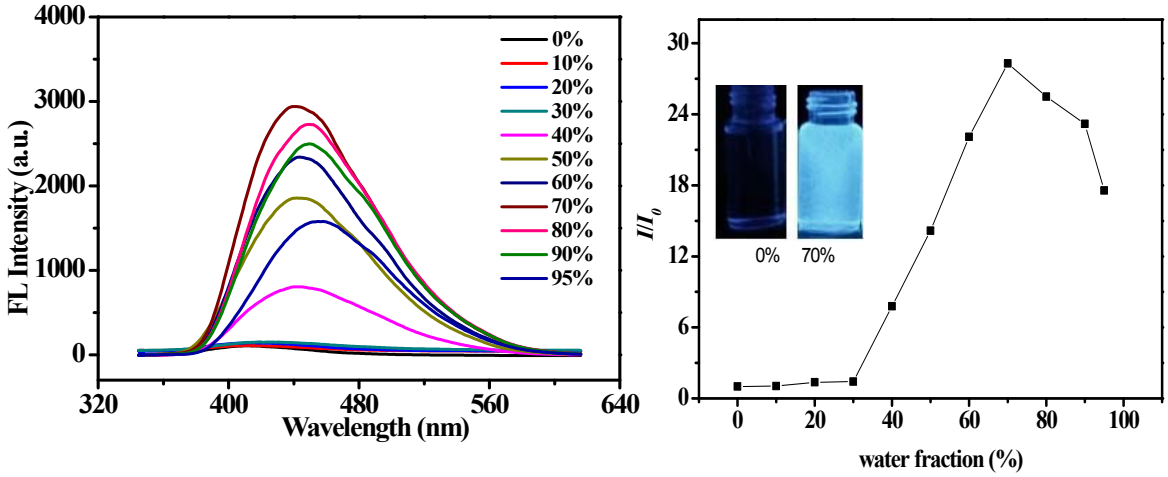

Figure S16 (left) The emission spectra of compound **3a** in H_2O/THF mixtures with different water fractions (λ_{ex} = 320 nm, 1.0×10^{-6} M); (right) The changes in peak intensities with different water fractions in H_2O/THF mixtures (I and I_o were the fluorescence intensities in H_2O/THF mixtures with different water fractions and in pure THF solution); Inserted: the corresponding fluorescence images.

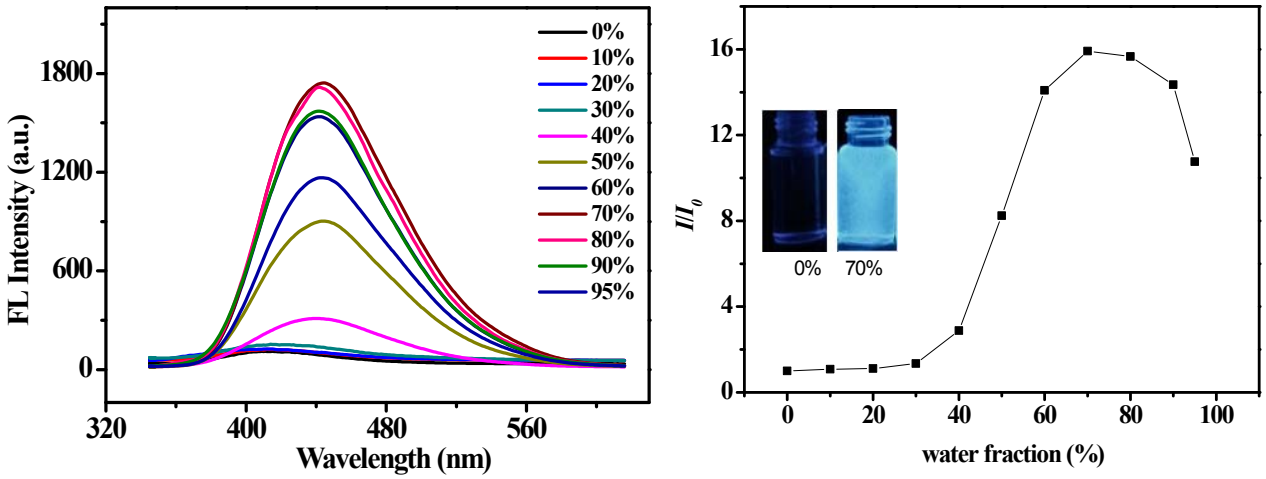

Figure S17 (left) The emission spectra of comp ound **3c** in H_2O/THF mixtures with different water fractions (λ_{ex} = 320 nm, 1.0×10^{-6} M); (right) The changes in peak intensities with different water fractions in H_2O/THF mixtures (I and I_o were the fluorescence intensities in H_2O/THF mixtures with different water fractions and in pure THF solution); Inserted: the corresponding fluorescence images.

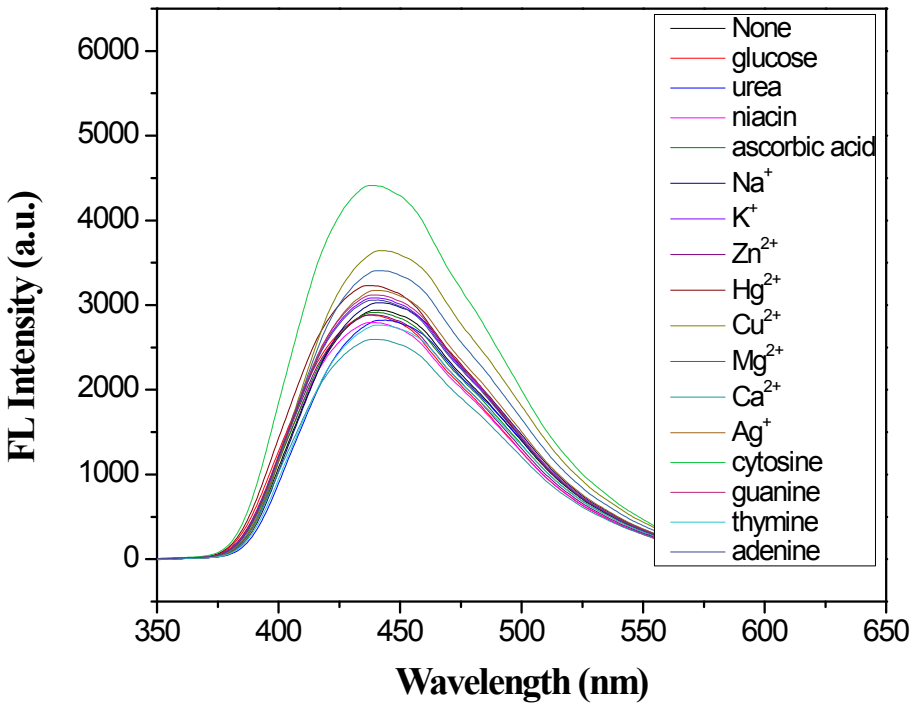

Figure S18 Fluorescence spectra of the compound **3a** in H_2O/THF mixtures with 70% of H_2O (λ_{ex} = 320 nm, 1.0×10^{-6} M) in the presence of various metal ions and biomolecules (1.0×10^{-6} M).

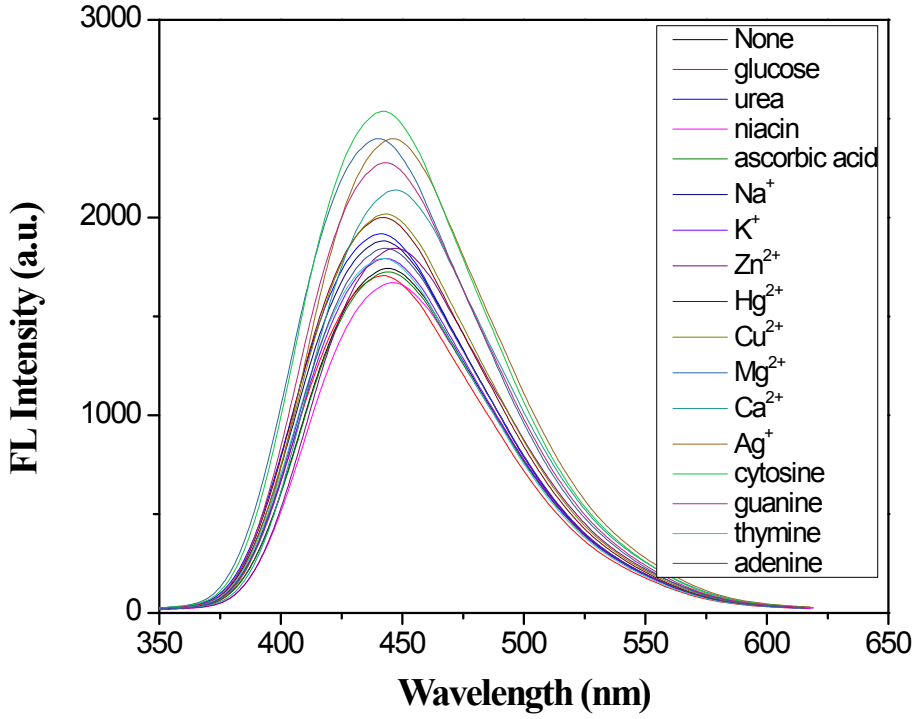

Figure S19 Fluorescence spectra of the compound **3c** in H_2O/THF mixtures with 70% of H_2O (λ_{ex} = 320 nm, 1.0×10^{-6} M) in the presence of various metal ions and biomolecules (1.0×10^{-6} M).

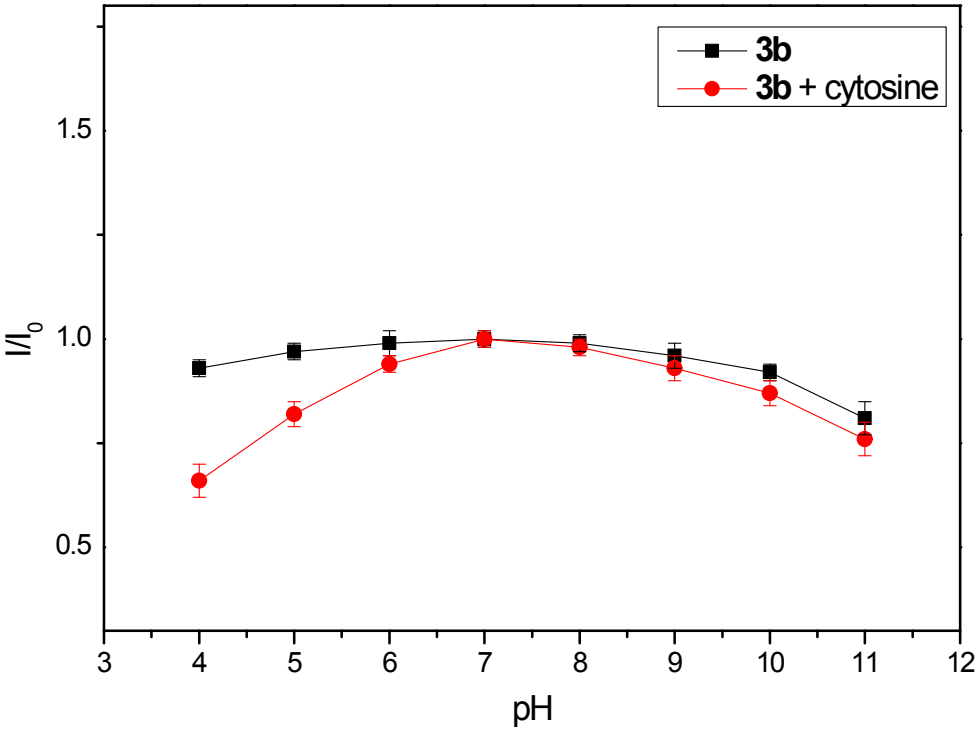

Figure S20 The influence of pH on the maximum fluorescence intensities of **3b** and **3b** with cytosine in H_2O/THF mixtures with 70% of H_2O (λ_{ex} = 320 nm, 1.0×10^{-6} M). I_o was the fluorescence intensities of **3b** or **3b** with cytosine at pH = 7, I were the fluorescence intensities of **3b** or **3b** with cytosine at corresponding pH values.

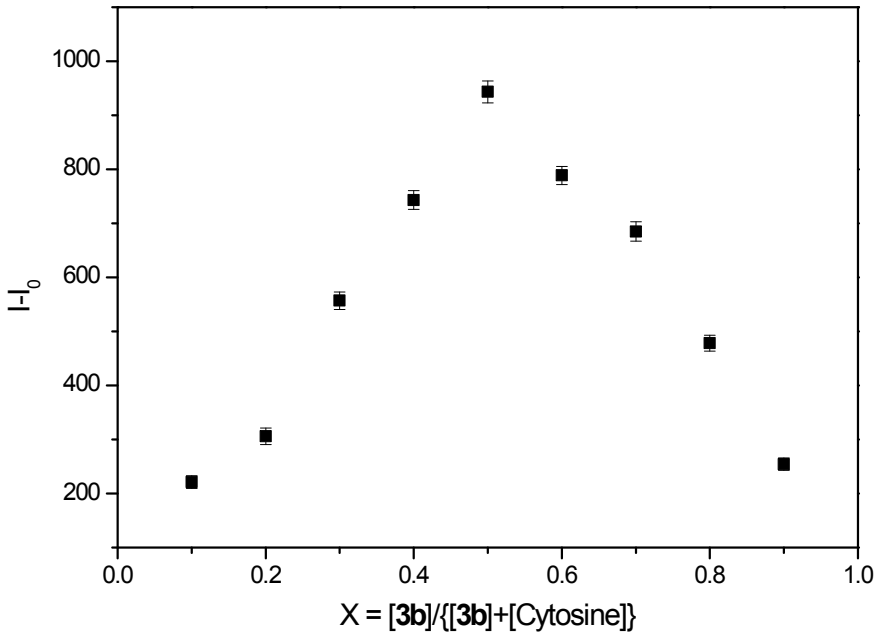

Figure S21 The Job's plot of compound **3b** with cytosine in H_2O/THF mixtures with 70% of H_2O (The total concentration was 1.0×10^{-6} M, I_0 and I were the fluorescence intensity of compound **3b** before and after sensing cytosine)

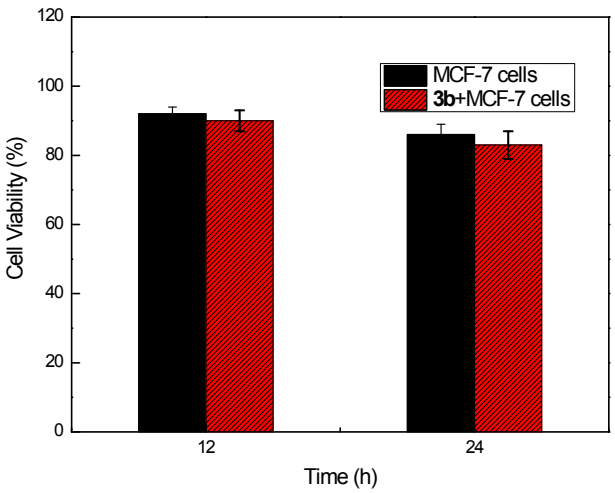

Figure S22 Cell viability of MCF-7 cells before and after incubated with compound **3b** (1.0×10^{-6} M) for 12 h and 24 h.

Table S1 Comparison of other methods for sensing cytosine

Method	LOD	Reference	Selectivity
Surface plasmon resonance sensor	10 nM	[22]	well
Electrocatalysis of uric acid	9.31 μM	[16]	well
Electroanalysis of functionalized graphene	0.23 μM	[17]	well
Glassy carbon electrode confined conducting polymer	65 nM	[18]	Not meentioned
Graphite-Based Nanocomposite Electrochemical Sensor	0.9 μM	[13]	weak
fluorescent DNA sensor	5.5 nM	[24]	Well
fluorescence sensor of thiophene-based organic nanoparticles	2.1 nM	[23]	weak
AIE fluorescence sensor	0.10 μM	This work	well

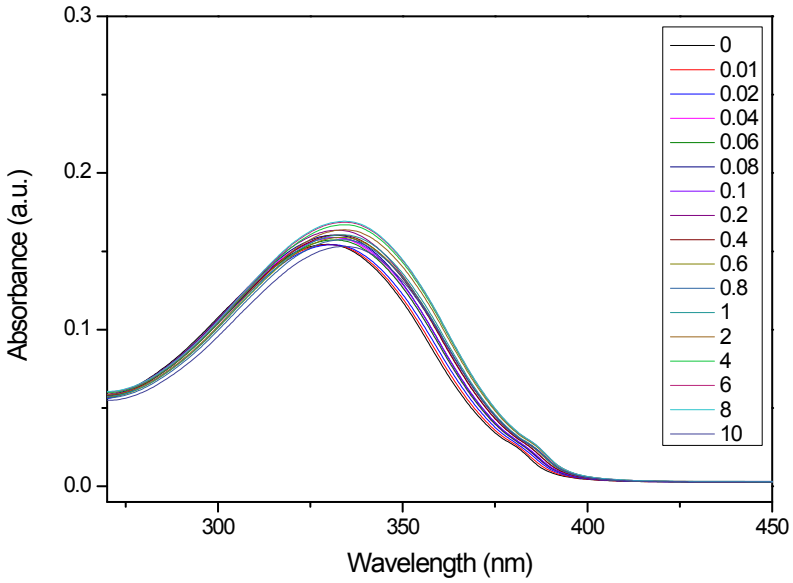

Figure S23 The UV-Vis absorption spectra of compound **3b** in H_2O/THF mixtures with 70% of H_2O (1.0×10^{-6} M) in the presence of various equivalent concentrations of cytosine.

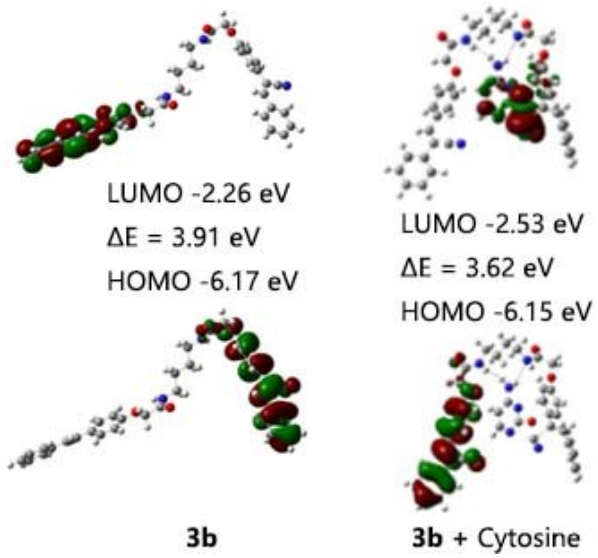

Figure S24 The Molecular theoretical orbital amplitude plots of HOMO and LUMO energy levels of compound **3b** before and after binding cytosine